Organic & Biomolecular Chemistry

PAPER

View Article Online
View Journal | View Issue

Cite this: *Org. Biomol. Chem.*, 2017, **15**, 8627

Highly selective recognition of Al^{3+} and I^- ions using a bi-functional fluorescent probe†

Zhao Li,‡[a] Jiang-Lin Zhao,‡[b] Yu-Tian Wu,[a] Lan Mu,[a] Xi Zeng,*[a] Zongwen Jin,*[b] Gang Wei,*[c] Ning Xie[d] and Carl Redshaw[e]

Received 14th September 2017,
Accepted 28th September 2017

DOI: 10.1039/c7ob02301d

rsc.li/obc

A tripodal fluorescent probe **L1** armed with Rhodamine B and 1-naphthaleneisothiocyanates was prepared in high yield. A study of the recognition properties revealed that probe **L1** exhibited high sensitivity and selectivity towards Al^{3+} through a "FRET" fluorescence response and colorimetric response with low detection limits of the order of 10^{-8} M. Meanwhile, probe **L1** also possessed high recognition ability for I^- through fluorescence decay, which given there are comparatively few selective fluorescent probes for I^-, is significant. Furthermore, the complexation mechanisms were fully investigated by spectral titrations, ^1H NMR spectroscopic titrations and mass spectrometry. The utility of probe **L1** as a biosensor in living cells (PC3 cells) towards Al^{3+} ions has also been demonstrated.

Introduction

Aluminum, the third most abundant element in the lithosphere, is widely used in our daily life typically in aluminum-based pharmaceutical drugs, food additives and kitchen utensils[1] as well as in different industries including paper, textile, and water treatment.[2] However, Al^{3+} is not necessary for the human body, and was found to be neurotoxic to living organisms. According to the Food and Agriculture Organization and World Health Organization Joint Expert Committee on Food Additives, the daily intake of Al^{3+} should not exceed 3–10 mg per day per kg body mass.[3] Indeed, an excessive intake of Al^{3+} into the human body may cause a variety of diseases such as myopathy, dementia, anemia, bone and joint diseases, as well as Alzheimer's and Parkinson's diseases.[4] Thus, the detection and quantification of Al^{3+} in environmental and living biosystems is of great importance.

On the other hand, iodine is a critical micronutrient in producing indispensable thyroid hormones in human thyroid glands, which play fundamental physiological roles at all stages of human development from fetus to adulthood.[5] However, either iodide deficiency or excessive intake can cause thyroid disorders. For example, a lack of sufficient iodine can typically lead to congenital anomalies, miscarriage and stillbirth.[6] In contrast, an excessive intake of iodine also results in negative effects, such as necrotic, degenerative, and neoplastic lesions in the thyroid gland, stomach and salivary glands.[7] Dasgupta has recently pointed out that nearly a third of the global population is suffering from insufficient iodine intake and is at risk of developing iodine deficiency disorders.[8] Therefore, the robust detection of iodide is highly desirable. Unfortunately, comparatively few selective fluorescent probes for I^- are currently available due to the iodide ion exhibiting the weakest binding capacity towards abiotic receptors owing to its large size *versus* other anions and poorest basicity amongst all the halide ions.[9] At the same time, the iodine ion is a fluorescence quenching heavy atom. Therefore, designing satisfactory I^- sensors still remains a big challenge.

Fluorescent probes are widely used as powerful tools for detecting ions owing to their high sensitivity, selectivity, rapid response rate, simplicity of manipulation and their capacity for real-time imaging and non-destructive nature.[10] In particular, bi-functional probes, which refer to those based on a single host that can independently recognize two guest species using distinct spectral responses,[11] have already been reported and this is emerging as a promising research area. In view of the importance of quantification of the Al^{3+} and I^- ions, there is an urgent need to develop a bi-functional probe which has the ability to detect both Al^{3+} and I^-.

Herein, we introduce a tripodal bi-functional fluorescent probe (**L1**), which not only exhibits high selectivity for the Al^{3+}

[a]*Key Laboratory of Macrocyclic and Supramolecular Chemistry of Guizhou Province; School of Chemistry and Chemical Engineering, Guizhou University, Guiyang 550025, China. E-mail: zengxi1962@163.com*
[b]*Shenzhen Institutes of Advanced Technology, Chinese Academy of Sciences, 1068 Xueyuan Avenue, Shenzhen 518055, China*
[c]*CSIRO Manufacturing Flagship, PO Box 218, NSW 2070, Australia*
[d]*College of Life Sciences and Oceanography, Shenzhen Key Laboratory of Microbial Genetic Engineering, Shenzhen University, Shenzhen 518060, China*
[e]*Department of Chemistry, School of Mathematics and Physical Sciences, University of Hull, Hull HU6 7RX, UK*

†Electronic supplementary information (ESI) available: Details of ^1H, ^{13}C NMR and mass spectra of probe **L1**. See DOI: 10.1039/c7ob02301d

‡These authors contributed equally to this work.

cation based on the FRET mechanism, but also high selectivity for I^- anions based on fluorescence quenching accompanied by distinct colour changes. Moreover, fluorescence imaging experiments using live PC3 cells and the detection of intracellular Al^{3+} ions in living cells are also discussed herein.

Results and discussion

Synthesis

The tripodal probe **L1** was prepared following the reported procedure with minor revisions in order to improve the yield (Scheme 1).[12] Rhodamine B was reacted with a large excess (8 equiv.) of tris(2-aminoethyl)amine to give the intermediate **1** in 87.3% yield. Intermediate **1** was then coupled with two equiv. of 1-naphthaleneisothiocyanate in dry $CHCl_3$ at reflux overnight (24 h) to afford probe **L1** in 76.3% yield (*cf.* ref. 12, 46%). The structure of **L1** was fully elucidated by FT-IR, ^1H and ^{13}C NMR spectroscopy as well as mass spectrometry (Fig. S1–S6†).

Recognition properties of probe L1 towards cations

Both fluorescence and UV-vis absorption spectroscopy were employed herein to investigate the recognition properties of probe **L1**. In H_2O/CH_3CN (10 μM, 2/98, v/v, pH = 7) solution, the fluorescence response of **L1** toward different metal ions was tested by exciting at 240 nm. Upon the addition of 20 equiv. of various ions (Li^+, Na^+, K^+, Ag^+, Mg^{2+}, Ca^{2+}, Ba^{2+}, Sr^{2+}, Hg^{2+}, Pb^{2+}, Cd^{2+}, Zn^{2+}, Co^{2+}, Ni^{2+}, Cu^{2+}, Fe^{3+} and Al^{3+}), only Al^{3+} exhibited an obvious emission change with a large Stokes shift (a dramatic fluorescence enhancement at 585 nm was observed, $\Delta\lambda$ = 345 nm), whereas the remaining other ions had no significant response on the fluorescence emission spectra of **L1**. It strongly suggested that **L1** possessed a specific response towards Al^{3+} ions (Fig. 1a).

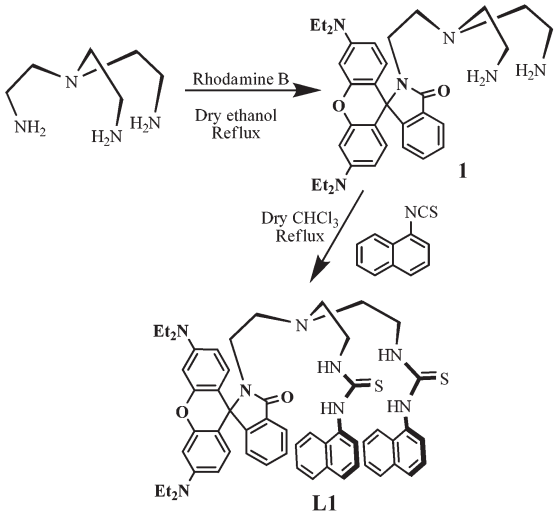

Scheme 1 The synthetic route to probe **L1**.

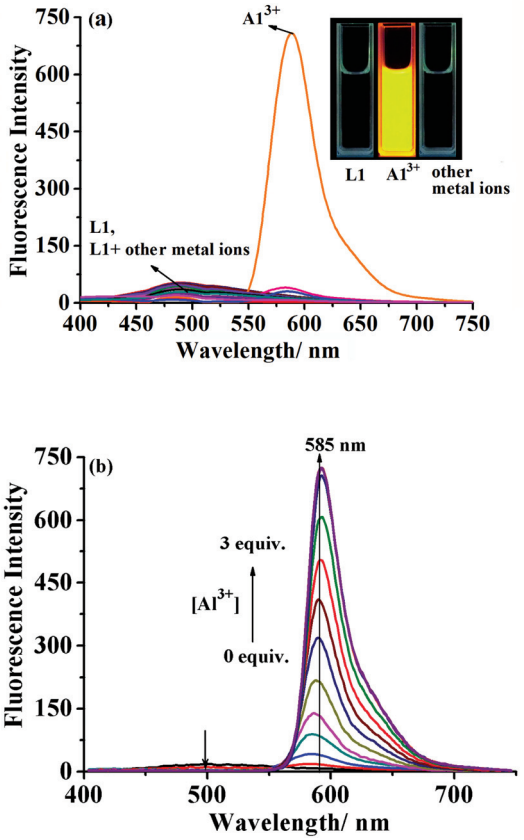

Fig. 1 (a) Fluorescence spectra of probe **L1** (10 μM, pH 7, H_2O/CH_3CN, 2/98, v/v) with 20 equiv. of different metal ions (inset shows the colour change of probe **L1** in the absence and the presence of Al^{3+} under UV-vis light); (b) fluorescence spectral changes of probe **L1** (50 μM, pH 7, H_2O/CH_3CN, 2/98, v/v) solution upon addition of Al^{3+} (0–3 equiv.). $\lambda_{ex}/\lambda_{em}$ = 240 nm/585 nm.

Fluorescence titration experiments were performed to investigate the detailed complexation process of probe **L1** with Al^{3+} (Fig. 1b). In the absence of metal ions, probe **L1** only exhibited a weak excimer emission peak ($\lambda_{ex}/\lambda_{em}$ = 240 nm/495 nm, the quantum yield Φ = 0.012 *versus* quinine sulfate as a reference material, Φ = 0.56, Fig. S7a†). This can be attributed to the tertiary N atom in the tren fragment of **L1**, which provides an unshared electron pair, and would quench the monomer and excimer emissions of the naphthalene moiety by a PET process. Meanwhile, the Rhodamine is present in its spirolactam state and suppresses the energy transfer from the excited naphthalene moiety to lactonized Rhodamine.[13] Upon increasing the concentration of Al^{3+}, the naphthalene excimer emission maximum at 495 nm was completely quenched. At the same time, a typical Rhodamine emission band centered at 585 nm with a 32.5-fold enhancement was observed (Φ = 0.39) which suggested that an efficient FRET process takes place from the donor (naphthalene) group to the acceptor (Rhodamine) group. This could be attributed to the chelation of Al^{3+} with the oxygen, sulfur atoms and the thiourea moiety resulting in inhibition of the PET process, whilst inducing the

Rhodamine spirolactam ring-opening of **L1**. Consequently, the increased overlap between the emission of the energy donor and absorption of the energy acceptor led to the intramolecular FRET (Fig. S8†).[13] The FRET efficiency between the donor and acceptor moieties was calculated to be 71% by the literature method.[14] The spectral changes were almost complete upon the addition of 2 equiv. of Al^{3+}, consistent with the molar ratio (Fig. S9a†). The 1 : 2 **L1**·$2Al^{3+}$ complex stoichiometry was further confirmed by a Job's plot (Fig. S9b†).

Similar selectivity was also observed in the UV-vis absorption spectra (Fig. 2). Following the addition of 20 equiv. of various cations, only the addition of Al^{3+} resulted in an acute absorption band centered at 555 nm, which clearly indicated the complexation of Al^{3+} and the formation of a ring-opened structure for the Rhodamine moiety. The visible colour change from colourless to pink also supported the tunable 'close–open' Rhodamine spirolactam structure (Fig. 2 inset).[15] Furthermore, this remarkable colour change can be employed to conveniently distinguish Al^{3+} by the naked eye. Although there was a slight absorption at 558 nm in the presence of Hg^{2+}, Cu^{2+}, Pb^{2+} and Fe^{3+} ions, it did not create any significant interference for the detection of Al^{3+} (Fig. 3), which was consistent with the fluorescence result (Fig. S10†).

UV-vis absorption titration experiments were also employed to investigate the binding process of **L1** towards Al^{3+}. As shown in Fig. S13a,† a new absorption band at 558 nm, which gradually increased upon the addition of Al^{3+} was observed, and this reached equilibrium at 2 equiv. of Al^{3+} (Fig. S13b†). This suggested a 1 : 2 binding ratio, which was further supported by a Job's plot analysis (Fig. S13c†) for this complexation. These results are consistent with the fluorescence analysis results (Fig. S9†). The 1 : 2 ratio of the **L1**·$2Al^{3+}$ complex was further confirmed by MALDI-TOF mass spectrometry. A mass peak at *m*/*z* 989.43021 (calculated value 989.39114) was observed which corresponded to $[\mathbf{L1} + 2Al - 5H]^+$, strongly suggestive of the formation of a 1 : 2 complex (Fig. S14†).

The binding mode of **L1** with Al^{3+} was examined by ^1H NMR spectroscopy in $CD_3CN/CDCl_3$ (4/6, v/v). The partial ^1H NMR spectra of **L1** before and after treatment with various concentrations of $Al(ClO_4)_3$ are shown in Fig. 4. The presence of Al^{3+} can affect the proton signals which are close to the Al^{3+} binding site. The ring proton signals of Rhodamine were

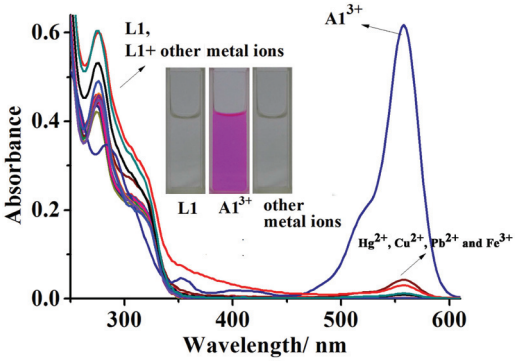

Fig. 2 Absorption spectra of probe **L1** (10 μM, H_2O/CH_3CN, 2/98, v/v, pH 7) with 20 equiv. of different metal ions. Inset shows the colour change of probe **L1** in the absence and the presence of Al^{3+} under day light, λ_{max} = 558 nm.

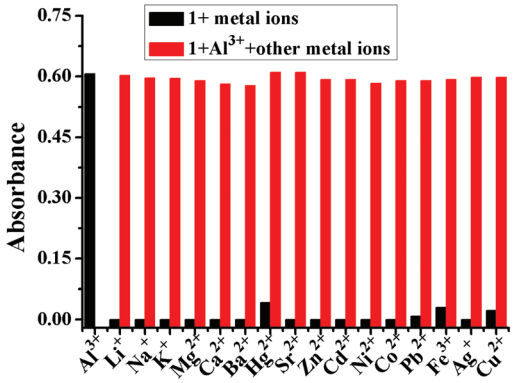

Fig. 3 Absorption response of probe **L1** (10 μM, H_2O/CH_3CN, 2/98, v/v, pH 7). Black bars: The absorbance of probe **L1** at 558 nm on addition of the respective metal ions (20 equiv.). Red bars: The absorbance of **L1**·$2Al^{3+}$ complex at 558 nm on addition of the respective competing metal ions (20 equiv.). Metal ions including Al^{3+}, Li^+, Na^+, K^+, Mg^{2+}, Ca^{2+}, Ba^{2+}, Sr^{2+}, Hg^{2+}, Pb^{2+}, Cd^{2+}, Zn^{2+}, Co^{2+}, Ni^{2+}, Cu^{2+}, Ag^+ and Fe^{3+}.

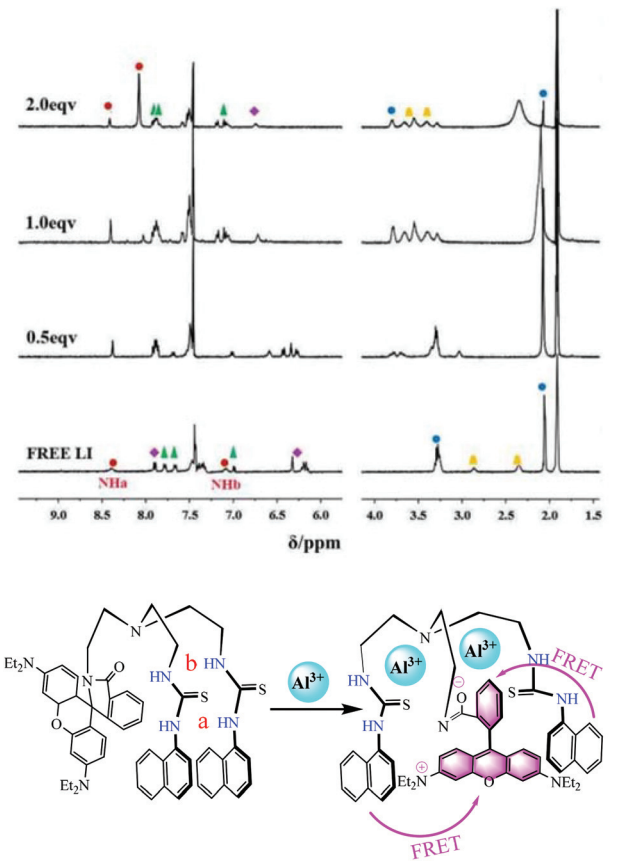

Fig. 4 (Up) Partial ^1H NMR spectra of probe **L1** (5 mM) and increasing concentrations of Al^{3+} in $CD_3CN/CDCl_3$ (4/6) solution at 298 K; (bottom) possible binding model of the probe **L1** with Al^{3+} ion complexes.

shifted downfield and broadened and gradually disappeared upon the addition of Al^{3+}. This indicated the opening of the spirolactam ring upon coordination to Al^{3+} with associated charge transfer at the xanthene moiety. At the same time, the methylene protons of the tren moiety also shifted downfield, which strongly suggested that Al^{3+} was bound to the nitrogen atoms of the tren. In addition, the aromatic protons of the naphthyl thiourea were only slightly shifted downfield ($\Delta\delta$ = 0.016–0.214 ppm, respectively) given the involvement of the thiourea sulfur atoms in the Al^{3+} binding process. The latter resulted in the decrease of electron density at these moieties which also resulted in the NH thiourea protons being shifted downfield ($\Delta\delta$ = 0.023–0.992 ppm, respectively). These observations suggested that the Al^{3+} was bound to probe **L1** through one oxygen atom of a carbonyl group, nitrogen atoms of tren and sulfur atoms of thiourea. Consequently, combined with the UV and fluorescence assay results, we proposed the possible binding model shown in Fig. 4 (bottom).

Recognition properties of probe L1 towards anions

Thiourea subunits are widely used in the design of neutral receptors for anions, owing to their ability to act as H-bonding donors.[16] Hence, we also investigated the sensing properties of **L1** towards different anions by fluorescence, absorption and ^{1}H NMR spectroscopy.

In 1,4-dioxane/water (v/v, 99/1) solution, probe **L1** (10 μM, Fig. 5a) exhibited absorption peaks at 274 nm and 310 nm, which corresponded to the π → π* and n → π* transitions of the naphthalene groups, respectively.[12] Upon the addition of 20 equiv. of various anions, *viz.* F^-, Cl^-, Br^-, NO_3^-, $H_2PO_4^-$, HSO_4^-, ClO_4^-, AcO^- and PF_6^-, there were no detectable changes, except in the case of I^-, which indicated the high selectivity of **L1** for I^- anions. Two new absorption peaks at 295 nm and 360 nm appeared in the presence of 20 equiv. of I^- ions, which suggested the formation of an **L1**·I complex. Furthermore, UV titration experiments revealed the details of the complexation process; the new absorption peaks at 295 nm and 360 nm gradually enhanced upon increasing the amount of I^- (Fig. S17†). However, no detectable absorption for the Rhodamine moiety (*e.g.* absorption band at 558 nm) was observed, which indicated that the Rhodamine moiety did not contribute to the complexation process. Moreover, the characteristic absorptions for the naphthalene group (274 nm and 310 nm) were unchanged. Consequently, we speculate that the new absorption peaks at 295 nm and 360 nm can be attributed to the formation of a new intramolecular hydrogen bond, leading to the formation of two six-membered rings *via* hydrogen bonding with the I^- anion (Fig. 5d).

We then further employed the fluorescence method to analyze the recognition properties of probe **L1** towards anions. Similar selectivity was observed by using fluorescence analysis, namely probe **L1** exhibited a high selectivity for I^- as evidenced by a fluorescence decrease (Fig. 5b). According to the fluorescence titration experiments, only the excimer emission was observed, *i.e.* no detectable monomer emission can be observed (Fig. S19†). This indicated the formation of hydro-

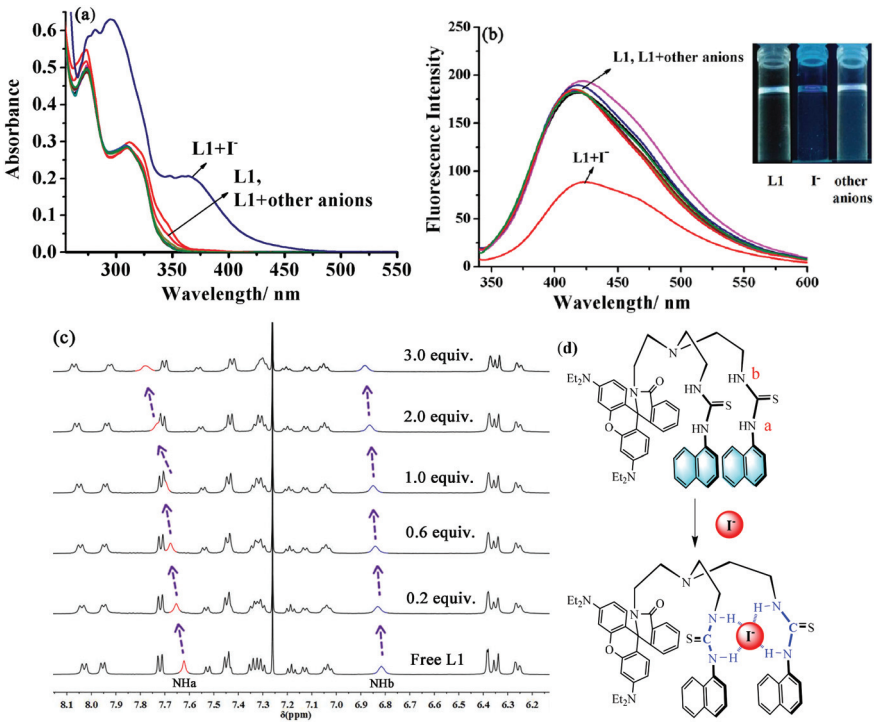

Fig. 5 Absorption (a) and fluorescence (b) spectra of probe **L1** (10 μM, 1,4-dioxane/H_2O, v/v, 99/1) with different anions (200 μM). Anions: I^-, F^-, Cl^-, Br^-, NO_3^-, $H_2PO_4^-$, HSO_4^-, ClO_4^-, AcO^-, PF_6^-. λ_{ex} = 310 nm; (c) partial ^{1}H NMR spectra of probe **L1** (5 mM) and increasing concentrations of I^- in $CDCl_3$ solution at 298 K; (d) proposed binding model of the probe **L1** with I^- ion complexes.

gen-bonding between the I^- ion and the NH of the two thiourea moieties and diminished the π–π stacking interaction between the two naphthalenes.

In order to confirm our speculation and to obtain additional information about the coordination mode of **L1** with I^-, ^1H NMR titration experiments were performed in $CDCl_3$ (Fig. 5c). Both the N*H*a and N*H*b protons were shifted downfield ($\Delta\delta$ 0.153 ppm and 0.065 ppm, respectively) upon the addition of 3.0 equiv. of I^-, which strongly suggested that the thiourea N*H* protons were interacting with I^-. Furthermore, the doublet signals of the naphthyl ring were also shifted slightly downfield. These observations suggested that the complexation between **L1** and the I^- anion occurs *via* multiple hydrogen bonding. Additionally, both the UV spectra and the fluorescence Job's plot analysis revealed a 1 : 1 stoichiometry (Fig. S18 & S20†). Consequently, we proposed the possible binding mode as shown in Fig. 5d, where the I^- ion was fixed in the middle of the two 1-naphthyl isothiocyanate moieties through hydrogen bonds which diminished the π–π stacking interaction between the two naphthalenes and resulted in the observed decreased fluorescence.

To further investigate the practical applicability of probe **L1** (10 μM) as an I^- ion selective fluorescent probe, competitive anion experiments were carried out in the presence of I^- mixed with 50 equiv. of the coexisting anions F^-, Cl^-, Br^-, I^-, HSO_4^-, NO_3^-, ClO_4^-, PF_6^-, AcO^- and $H_2PO_4^-$ in 1,4-dioxane/water (v/v, 99/1) solution. As shown in Fig. S21,† no interference in the detection of I^- with probe **L1** was observed in the presence of these other competitive anions. Accordingly, these observations strongly suggested that probe **L1** can serve as a selective probe for I^- in the presence of the above-mentioned ions for real life applications.

The detection of linear relationships and limits of detection (LOD = 3σ/slope) for probe **L1** with Al^{3+} and I^-, under the optimal conditions, are summarized in Table 1 (Fig. S11, S12, S15, S16 & S22–S25†). A relatively wide linear range can be calculated which will allow for more convenient/widespread detection applications. The LOD of probe **L1** towards the cation Al^{3+}, and the anion I^- was of the order of 10^{-8} M by fluorescence or 10^{-6} M by the colorimetric method, which is far below most previously reported systems (Table S1†).[17] This data strongly suggest that the probe **L1** is a sensitive dual function sensor for the detection of Al^{3+} and I^-.

Cell imaging study

The ability of probe **L1** to detect Al^{3+} within living cells was investigated by fluorescence imaging on a fluorescence inverted microscope. The prostate cancer (PC3) cells were incubated with probe **L1** (20 μM) in RPMI medium for 40 min at 37 °C and washed with fresh RPMI medium to remove any excess of probe **L1**. No intracellular fluorescence was monitored in the bright-field image (Fig. 6a) and in the fluorescence image (Fig. 6b). The incubated cells were then further treated with 100 μM of Al^{3+} for 40 min, and a dramatic intracellular fluorescence was observed (Fig. 6c and d). It unambiguously confirmed that the red or green fluorescence was induced by the response of probe **L1** towards the intracellular Al^{3+} ions. The strong red or green fluorescence emission indicated a

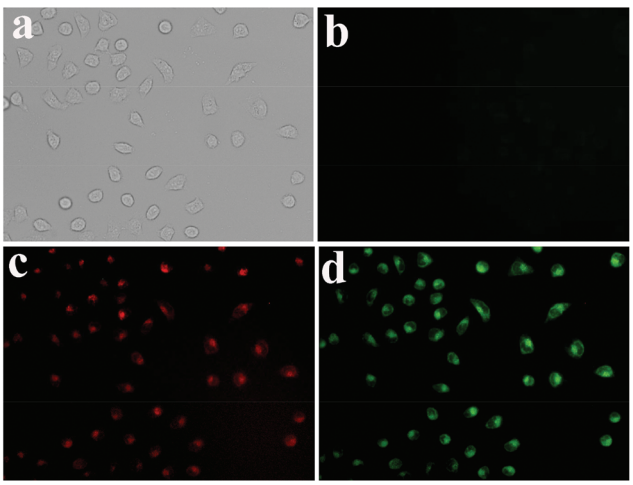

Fig. 6 Fluorescence images of PC3 cells: (a) bright-field image of cells after incubation with probe **L1** (20 μM); (b) fluorescence image of (a) in red or green channel; (c) fluorescence images of PC3 cells incubated with probe **L1** (20 μM) for 40 min, then treated with Al^{3+} (100 μM) for 40 min in the red channel; (d) fluorescence images of (c) in green channel; red channel: λ_{ex} = 510 nm–550 nm; green channel: λ_{ex} = 450 nm–490 nm.

Table 1 Analysis parameters for **L1** and detection of Al^{3+} and I^-

Method		The linear range of the calibration curve (μM)	Correlation coefficient	LOD ($\times 10^{-8}$ M)	Association constants K_a
Fluorescence	Al^{3+}	16.7–95	0.9935	6.2	K_1 = 777.45 (±0.391) M^{-1} $K_2 = 3.099 \times 10^5$ (±0.391) M^{-1} R = 0.9898
	I^-	1–500	0.9953	9.2	$K_a = 1.04 \times 10^4$ (±0.033) M^{-1} R = 0.9910
Absorption	Al^{3+}	10.5–95	0.9055	580	K_1 = 1225.8 (±0.312) M^{-1} $K_2 = 2.654 \times 10^5$ (±0.312) M^{-1} R = 0.9842
	I^-	2.0–480	0.9578	42	$K_a = 2.08 \times 10^5$ (±0.005) M^{-1} R = 0.9975

high permeability of probe **L1** into living cells, which can be applied for the monitoring of intracellular Al^{3+} in PC3 cells by *in vitro* imaging and also potentially by *in vivo* methods.

Conclusions

In summary, Rhodamine B and 1-naphthaleneisothiocyanate were employed here to construct the tripodal probe **L1**, which possessed the ability for forming a FRET probe due to fluorescence spectra overlap. The recognition properties of probe **L1** were fully investigated by fluorescence, absorption and ^{1}H NMR spectroscopic titration and mass spectrometry. For the cation recognition study, probe **L1** exhibited high sensitivity and selectivity towards Al^{3+} through a "FRET" fluorescence response with a large Stokes shift and colorimetric response with low detection limits of 7.3×10^{-8} M. On the other hand, the anion recognition study revealed that probe **L1** also possessed high sensitivity (4.6×10^{-7} M) and selectivity towards I^- observed *via* a decrease in fluorescence. This is a significant addition to the number of detection assays available for I^-, particularly as there are comparatively few selective fluorescent probes for I^-. Additionally, probe **L1** has been exploited for the detection of Al^{3+} in living cells. The successful fluorescence imaging experiments suggested that probe **L1** possessed good permeability into living cells, which can be applied for monitoring intracellular Al^{3+} in PC3 cells by *in vitro* imaging and also potentially by *in vivo* methods. This work provides a promising strategy for the detection of metal ions and anionic species in biological and environmentally relevant systems.

Experimental

Materials and methods

Unless otherwise stated, all reagents used were purchased from commercial sources and were used without further purification. The solutions of the metal ions were prepared from their nitrate salts (Aldrich and Alfa Aesar Chemical Co., Ltd). All the anions used were tetra-*n*-butylammonium salts (Sigma-Aldrich Chemical Co.), and were stored in a desiccator under vacuum containing self-indicating silica. Other chemicals used in this work were of analytical grade and were used without further purification. Double distilled water was used throughout. Fluorescence spectral measurements were performed on a Cary Eclipse fluorescence spectrophotometer (Varian) equipped with a xenon discharge lamp using a 1 cm quartz cell. UV-Vis absorption spectra were recorded on a UV-1800 spectrophotometer (Shimadzu) in a 1 cm quartz cell. IR spectra were obtained using a Vertex 70 FT-IR spectrometer (Bruker). ^{1}H and ^{13}C NMR spectra were recorded on a JEOL JNM-ECZ400S 400 MHz NMR spectrometer (JEOL) and a WNMR-I 500 MHz NMR spectrometer (Wuhan Institute of Physics and Mathematics, Chinese Academy of Sciences) respectively at room temperature using TMS as an internal standard. ESI-MS spectra were recorded on a Q Exactive spectrometer (Thermo). MALDI-TOF mass spectra were recorded on a BIFLEX III ultra-high resolution Fourier transform ion cyclotron resonance (FT-ICR) mass spectrometer (Bruker) with α-cyano-4-hydroxycinnamic acid as a matrix. Microelectrode layers using the sputtering and lift-off process with the standard photo-lithography (EVG 610, Austria). Cell fluorescence imaging was performed using a Ti (Nikon) fluorescence inverted phase contrast microscope.

Syntheses

Synthesis of intermediate 1. A mixture of tris(2-aminoethyl) amine (4.0 g, 27.36 mmol) and Rhodamine B (1.638 g, 3.42 mmol) in dry ethanol (60 mL) was refluxed for 24 h under an N_2 atmosphere. The solvent was removed by evaporation. The residue was extracted with CH_2Cl_2 (100 mL) three times, washed with water and dried with $MgSO_4$ overnight. The CH_2Cl_2 solvent was removed by evaporation and gave a light red oil product. The crude product was purified by column chromatography ($MeOH/CHCl_3/NEt_3$ = 9/1/1, v/v) to give 1.71 g colourless oil pure product **1** in 87.3% yield. ^{1}H NMR (500 MHz, $CDCl_3$) δ ppm 7.89 (d, J = 5.0 Hz, 1H, ArH), 7.44–7.46 (br, 2H, Ar*H*), 7.10 (bs, 1H, Ar*H*), 6.40–6.42 (m, 4H, Ar*H*), 6.27 (d, J = 5.0 Hz, 2H, Ar*H*), 3.34 (q, J = 10.0 Hz, 8H, NC*H*$_2$CH$_3$), 3.15 (m, 2H, NC*H*$_2$CH$_2$N), 2.55–2.57 (m, 4H, NC*H*$_2$CH$_2$N), 2.36 (t, J = 5.0 Hz, 4H, NC*H*$_2$CH$_2$N), 2.24 (t, J = 5.0 Hz, 4H, NC*H*$_2$CH$_2$N), 1.17 (t, J = 10.0 Hz, 12H, NCH$_2$C*H*$_3$); ^{13}C NMR (125 MHz, $CDCl_3$) δ 12.16, 37.51, 38.54, 43.96, 51.29, 54.79, 56.91, 97.23, 104.97, 107.71, 122.25, 123.43, 127.79, 128.47, 131.08, 132.03, 148.41, 152.55, 153.11, 167.41 ppm.

Synthesis of probe L1. A mixture of intermediate **1** (1.16 g, 2.03 mmol) and 1-naphthyl isothiocyanate (740 mg, 4.00 mmol) in dry $CHCl_3$ (120 mL) was refluxed overnight under an N_2 atmosphere. The solvent was removed by evaporation. The residue was extracted with CH_2Cl_2 (100 mL) three times, washed with water and dried with $MgSO_4$ overnight. The CH_2Cl_2 solvent was removed by evaporation. The crude product was purified by column chromatography (EtOAc/hexane = 7/3, v/v) to give 1.45 g of white solid **L1** in 76.3% yield. M.p. 125–127 °C; IR (KBr, ν cm^{-1}): 3333 (N–H), 1603 (C=C), 1518 (C–N–H), 1103 (C–O), 772 (Ar–H), 625 (Ar–H). ^{1}H NMR (500 MHz, $CDCl_3$) δ: 8.13 (s, 2 H, CS*NH*), 7.92 (d, J = 8.0 Hz, 2 H, Ar*H*), 7.79 (d, J = 8.0 Hz, 2 1H, Ar*H*), 7.67 (d, J = 8.0 Hz, 2 H, Ar*H*), 7.61 (d, J = 8.0 Hz, 2 H, Ar*H*), 7.27–7.48 (m, 9 H, Ar*H*), 7.12–7.24 (s, 2 H, CS*NH*), 7.09 (d, J = 8.0 Hz, 2 H, Ar*H*), 6.38 (d, J = 4.0 Hz, 2H, Ar*H*), 6.21–6.27 (m, 4H, Ar*H*), 3.25–3.41 (m, 12 H, NC*H*$_2$CH$_3$ & NHCH$_2$), 2.84–2.87 (t, 2 H, NC*H*$_2$CH$_2$N), 2.35–2.39 (t, 4 H, NC*H*$_2$CH$_2$N), 1.92–1.94 (t, 2H, NC*H*$_2$CH$_2$N), 1.07–1.18 (m, 12 H, NCH$_2$C*H*$_3$); ^{13}C NMR (500 MHz, $CDCl_3$) δ 12.56, 37.72, 40.24, 44.41, 53.55, 54.33, 66.81, 97.67, 104.66, 108.48, 118.01, 121.10, 122.68, 123.18, 124.08, 125.49, 125.58, 126.07, 126.63, 128.38, 128.44, 128.70, 131.02, 133.00, 134.09, 134.52, 149.03, 152.86, 153.62, 156.62, 169.55 ppm; MS (MALDI-TOF) calcd for $[C_{56}H_{60}N_8O_2S_2]$: m/z 940.42806, found: m/z 941.17524 $[M + H]^+$.

Spectral measurement

To a 10 mL volumetric flask containing different amounts of ions, appropriate amounts of the solution of probe **L1** were

added using a micropipette. For Al^{3+}, the system was then diluted with CH_3CN/H_2O (49/1, v/v) mixed solvent to 10 mL; for I^-, it was diluted with 1,4-dioxane/water (v/v, 99/1) to 10 mL, and then the fluorescence and absorption sensing of the ions was conducted. The fluorescence and UV-vis spectra were recorded after the addition of the ions at room temperature and when equilibrium was reached. Fluorescence measurements were carried out with an excitation and emission slit width of 10 nm.

Cell culture and fluorescence imaging

PC3 cells were grown using a modified Roswell Park Memorial Institute Medium supplemented with 10% fetal bovine serum, 100 U mL^{-1} penicillin and 100 μg mL^{-1} streptomycin at 37 °C and 5% CO_2. One day prior to imaging, the cells were seeded in 6-well flat-bottomed plates. The next day, the cells were incubated with 20 μM of probe **L1** for 40 min at 37 °C. Before incubating with 100 μM $Al(ClO_4)_3$ for another 40 min, the cells were rinsed with fresh culture medium three times to remove the remaining sensor, and then the fluorescence imaging of intracellular Al^{3+} was observed under an inverted fluorescence microscope excited with UV light.

Conflicts of interest

There are no conflicts of interest to declare.

Acknowledgements

This work was supported by the "Chun-Hui" Fund of Chinese Ministry of Education (no. Z2015007 & Z2016008), the SIAT Innovation Program for Excellent Young Researchers (2017014), the Natural Science Foundation of China (no. 21405170), the Basic Research Program of Shenzhen (no. JCYJ20150525092940997 & no. JCYJ20150521094519497), the Technology Research Program of Shenzhen (no. JSGG20160429184803117) and the Science and Technology Project of Guangdong (no. 2016B020238003). The EPRSC is thanked for financial support (Overseas Travel award to CR).

Notes and references

1 (*a*) A. Sahana, A. Banerjee, S. Lohar, A. Banik, S. K. Mukhopadhyay, D. A. Safin, M. G. Babashkina, M. Bolte, Y. Garcia and D. Das, *Dalton Trans.*, 2013, **42**, 13311–13314; (*b*) D. Maity and T. Govindaraju, *Chem. Commun.*, 2010, **46**, 4499–4501.

2 (*a*) W. S. Miller, L. Zhuang, J. Bottema, A. J. Wittebrood, P. D. Smet, A. Haszler and A. Vieregge, *Mater. Sci. Eng., A*, 2000, **280**, 37–49; (*b*) G. Ciardelli and N. Ranieri, *Water Res.*, 2001, **35**, 567–572; (*c*) R. A. Yokel, C. L. Hicks and R. L. Florence, *Food Chem. Toxicol.*, 2008, **46**, 2261–2266.

3 D. Sarkar, P. Ghosh, S. Gharami, T. K. Mondal and N. Murmu, *Sens. Actuators, B*, 2017, **242**, 338–346.

4 (*a*) B. Liu, P. F. Wang, J. Chai, X. Q. Hu, T. Gao, J. B. Chao, T. G. Chen and B. S. Yang, *Spectrochim. Acta, Part A*, 2016, **168**, 98–103; (*b*) N. Chatterjee, S. B. Maity, A. Samadder, P. Mukherjee, A. R. Khuda-Bukhsh and P. K. Bharadwaj, *RSC Adv.*, 2016, **6**, 17995–18001; (*c*) L. K. Kumawat, N. Mergu, M. Asif and V. K. Gupta, *Sens. Actuators, B*, 2016, **231**, 847–859; (*d*) Z. C. Liao, Z. Y. Yang, Y. Li, B. D. Wang and Q. X. Zhou, *Dyes Pigm.*, 2013, **97**, 124–128.

5 S. Venturi, *Curr. Chem. Biol.*, 2011, **5**, 155–167.

6 A. S. Green and E. Pearce, *Nat. Rev. Endocrinol.*, 2012, **8**, 650–658.

7 S. Venturi, F. M. Donati, M. Venturi, A. Venturi, L. Grossi and A. Guidi, *Adv. Clin. Pathol.*, 2000, **4**, 11–17.

8 C. P. Shelor and P. K. Dasgupta, *Anal. Chim. Acta*, 2011, **702**, 16–36.

9 S. Sandhu, R. Kumar, P. Singh, A. Walia, V. Vanita and S. Kumar, *Org. Biomol. Chem.*, 2016, **14**, 3536–3543.

10 (*a*) W. Sun, S. G. Guo, C. Hu, J. L. Fan and X. J. Peng, *Chem. Rev.*, 2016, **116**, 7768–7817; (*b*) E. Karakus, M. Ucuncu and M. Emrullahoglu, *Anal. Chem.*, 2016, **88**, 1039–1043; (*c*) S. Samanta, B. K. Datta, M. Boral, A. Nandan and G. Das, *Analyst*, 2016, **141**, 4388–4393; (*d*) H. Sui, Y. Wang, Z. Yu, Q. Cong, X. X. Han and B. Zhao, *Talanta*, 2016, **159**, 208–214; (*e*) Y. J. Chen, S. C. Yang, C. C. Tsai, K. C. Chang, W. H. Chuang, W. L. Chu, V. Kovalev and W. S. Chung, *Chem. – Asian J.*, 2015, **10**, 1025–1034.

11 S. K. Kim and J. L. Sessler, *Chem. Soc. Rev.*, 2010, **39**, 3784–3809.

12 C. Kaewtong, B. Pulpoka and T. Tuntulani, *Dyes Pigm.*, 2015, **123**, 204–211.

13 (*a*) C. Y. Li, Y. Zhou, Y. F. Li, X. F. Kong, C. X. Zou and C. Weng, *Anal. Chim. Acta*, 2013, **774**, 79–84; (*b*) M. H. Lee, H. J. Kim, S. Yoon, N. Park and J. S. Kim, *Org. Lett.*, 2008, **10**, 213–216; (*c*) A. B. Othman, J. W. Lee, J. S. Wu, J. S. Kim, R. Abidi, P. Thuéry, J. Marc Strub, A. V. Dorsselaer and J. Vicens, *J. Org. Chem.*, 2007, **72**, 7634–7640.

14 (*a*) G. W. Gordon, G. Berry, X. H. Liang, B. Levine and B. Herman, *Biophys. J.*, 1998, **74**, 2702–2713; (*b*) M. H. Lee, D. T. Quang, H. S. Jung, J. Y. Yoon, C. H. Lee and J. S. Kim, *J. Org. Chem.*, 2007, **72**, 4242–4245.

15 (*a*) H. Kim, S. Lee, J. Lee and J. Tae, *Org. Lett.*, 2010, **12**, 5342–5345; (*b*) X. C. Wang, J. Tao, X. Q. Chen and H. Yang, *Sens. Actuators, B*, 2017, **224**, 709–716; (*c*) K. B. Li, H. Wang, Y. Zang, X. P. He, J. Li, G. R. Chen and H. Tian, *ACS Appl. Mater. Interfaces*, 2014, **6**, 19600–19605.

16 (*a*) P. A. Gale, *Coord. Chem. Rev.*, 2001, **213**, 79–128; (*b*) P. D. Beer and P. A. Gale, *Angew. Chem., Int. Ed.*, 2001, **40**, 486–516.

17 (*a*) S. Erdemir, M. Yuksekogul, S. Karakurt and O. Kocyigit, *Sens. Actuators, B*, 2017, **241**, 230–238; (*b*) Y. Long, J. Zhou, M. Yang, X. J. Liu, M. Zhang and B. Q. Yang, *Sens. Actuators, B*, 2016, **232**, 327–335; (*c*) J. Liu and Y. Qian, *Dyes Pigm.*, 2017, **136**, 782–790.